DOI 10.1002/mnfr.201100677 *Mol. Nutr. Food Res.* 2012, *56*, 784–796

RESEARCH ARTICLE

Ellagitannin metabolites, urolithin A glucuronide and its aglycone urolithin A, ameliorate TNF-α-induced inflammation and associated molecular markers in human aortic endothelial cells

Juan A. Giménez-Bastida, Antonio González-Sarrías, Mar Larrosa, Francisco Tomás-Barberán, Juan C. Espín and María-Teresa García-Conesa

Research Group on Quality, Safety and Bioactivity of Plant Foods, Department of Food Science and Technology; CEBAS-CSIC , Murcia, Spain

Received: October 10, 2011
Revised: November 30, 2011
Accepted: December 21, 2011

Scope: Numerous in vitro and in vivo studies indicate that ellagitannins exhibit anti-inflammatory, anti-atherosclerotic and anti-angiogenic activity which support their potential preventive effect against cardiovascular diseases. Ellagitannins exhibit low bioavailability and are transformed in the gut to ellagic acid and its microbiota metabolites urolithin A (Uro-A) and urolithin B (Uro-B). Urolithins are found in plasma mostly as glucuronides at low μM concentrations. We investigated whether urolithin glucuronides and their aglycones exhibit vascular protective effects.

Methods and results: Human aortic endothelial cells were exposed to tumor necrosis factor alpha and to Uro-A glucuronide, Uro-B glucuronide or their corresponding aglycones at low μM concentrations to determine their effects on monocytes adhesion and endothelial cell migration. The levels of related adhesion cytokines and growth molecular markers were also measured. Uro-A glucuronide (∼5–15 μM) inhibited monocyte adhesion and endothelial cell migration in a significant manner. These effects were associated with a moderate but significant down-regulation of the levels of chemokine (C–C motif) ligand 2 (CCL2) and plasminogen activator inhibitor-1 (PAI-1). Uro-A inhibited endothelial cell migration and was able to decrease the expression of CCL2 and interleukin-8 (IL-8).

Conclusion: Our results suggest that these metabolites might be involved, at least in part, in the beneficial effects against cardiovascular diseases attributed to the consumption of ellagitannin-containing foods.

Keywords:
Angiogenesis / Atherosclerosis / Cell adhesion / Cell migration / Microbiota metabolites

1 Introduction

Atherosclerosis is the result of a chronic inflammatory condition of the vessel wall leading to vascular narrowing or obstruction, and is accompanied by vascular dysfunction [1]. It is driven by complex interactions between inflammatory cells and the vascular wall with the concurrence of an intricate network of stimulatory and signalling molecules [2]. Endothelial cells (ECs) lining the luminal surface of blood vessels play a vital role in maintenance of circulatory homeostasis including regulation of inflammatory responses, barrier function and angiogenesis [3]. Endothelial dysfunction

Correspondence: Dr. María-Teresa García-Conesa, Research Group on Quality, Safety and Bioactivity of Plant Foods, Department of Food Science and Technology, CEBAS-CSIC, P.O. Box 164, 30100 Campus de Espinardo, Murcia, Spain
E-mail: mtconesa@cebas.csic.es
Fax: +34-968-396213

Abbreviations: **CVDs**, cardiovascular diseases; **EA**, ellagic acid; **ETs**, ellagitannins; **HAECs**, human aortic endothelial cells; **PBS**, phosphate buffered saline; **TNF-α**, tumor necrosis factor alpha; **Uro-A**, urolithin A; **Uro-A-Gluc**, urolithin A glucuronide; **Uro-B**, urolithin B; **Uro-B-Gluc**, urolithin B glucuronide

and disrupted integrity of the ECs are characterized by an overexpression of pro-inflammatory and adhesion molecules as well as the release of different growth factors which represent a key early step in the development of atherosclerosis [4, 5]. The pro-inflammatory cytokine tumor necrosis factor alpha (TNF-α), largely produced by lymphocytes and activated monocytes/macrophages, is a crucial regulator of the inflammatory response in ECs and may underlie the vascular pathology in atherosclerosis and other cardiovascular diseases [6]. Among other activities, TNF-α induces the expression of adhesion molecules including intracellular adhesion molecule 1 (ICAM-1), vascular adhesion molecule 1 (VCAM-1), E-selectin (SELE) and monocyte chemoattractant protein-1 or chemokine (C–C motif) ligand 2 (MCP-1 or CCL2) which are crucial to the recruitment of monocytes to the vascular endothelium and their subsequent migration into the vessel [7].

Endothelial cell migration is critical to wound healing mechanisms that restore the normal integrity of endothelial cell lining of blood vessels and to angiogenesis, the process of blood vessels growth and proliferation which may also be important in the pathogenesis of atherosclerosis [8]. A regenerating and proliferative endothelium is a strong source of growth factors that form a complex signalling network that regulates the processes of wound healing and angiogenesis. Of particular importance are the epidermal growth factor (EGF) family, platelet-derived growth factor (PDGF) family or the transforming growth factor-beta (TGF-β) family [9]. TNF-α can also function as a pro-angiogenic molecule and can affect the proliferation and migration of ECs [10].

Endothelial dysfunction is a reversible process and strategies such as specific dietary antioxidants recommendations have been reported to prevent or reduce the risk of vascular dysfunction by inhibiting TNF-α production and (or) TNF-α-mediated responses (i.e., inflammation and angiogenesis) and consequently to reverse the atherosclerotic process [7]. Polyphenols are antioxidants abundant in plant foods and derived beverages which may provide an effective approach to improve vascular health [11]. Walnuts and pomegranate, rich in the phenolic antioxidants ellagitannins (ETs), have been associated with cardiovascular protective effects though *in vivo* evidence in animal or human intervention studies are limited. Numerous *in vitro* studies have shown anti-atherogenic, anti-inflammatory and anti-angiogenic effects of ETs and ellagic acid (EA) in cell models of the vascular system. However, these studies were poorly designed since, in most cases, cells of the vascular system were exposed to full plant extracts rich in ETs and (or) to rather high non-physiological concentrations of these compounds [12]. Instead, cells of the vascular system should be exposed to the metabolites derived from those original plant compounds and which are formed during the gastrointestinal digestion, microbiota metabolism and phase I and phase II metabolism [13]. In particular, ETs and EA are poorly absorbed and are further metabolized by the colonic microbiota to form mostly urolithin-A (Uro-A) and urolithin-B (Uro-B) as well as other minor urolithins [14]. The main metabolites detected in the plasma of humans after the intake of ET-containing foods were the glucuronides of Uro-A, Uro-B and Uro-C with total concentrations of these metabolites ranging from ∼0.2 μM up to ∼18.6 μM. These values show, however, a large variability between individuals and between days and thus, in one particular volunteer, it was found that the plasma values of Uro-B-Gluc and Uro-A-Gluc reached 10.8 and 6.7 μM, respectively [15, 16]. Since Uro-A has been reported to exert *in vitro* and *in vivo* anti-inflammatory properties in the colon [17, 18] we hypothesized that the circulating urolithin glucuronides may be, at least in part, the molecules responsible for some of the beneficial effects against cardiovascular diseases attributed to ET-containing foods.

With a view to elucidating the putative mechanisms by which dietary ETs may contribute to protect against inflammatory-based atherosclerotic early events, in the present study, we investigated some of the cellular and molecular responses associated with the exposure of TNF-α-activated human aortic endothelial cells (HAECs) to low μM concentrations of Uro-A-Gluc and Uro-B-Gluc. For comparative purposes, we also examined the effects of similar levels of their respective aglycones. We specifically explored the effects of these metabolites on: (i) monocyte adhesion to endothelial cells, (ii) endothelial cell migration and (iii) molecular markers involved in adhesion and migration (adhesion proteins and growth factors). In addition, we investigated the stability of the tested metabolites under the experimental cell culture conditions.

2 Materials and methods

2.1 Materials

Uro-A (3,8-dihydroxy-6H-dibenzo[b,d]pyran-6-one) and Uro-B (3-hydroxy-6H-dibenzo[b,d]pyran-6-one) were chemically synthesized by Kylolab S.A. (Murcia, Spain). Uro-B glucuronide, (Uro-B-Gluc, 3-hydroxy-6H-dibenzo[b,d]pyran-6-one glucuronide) was also chemically synthesized following a published procedure [19]. Supersomes expressing the recombinant human UDP glucuronosyltransferase 1 family, polypeptide A1 (UGT1A1) were obtained from BD Gentest (Woburn, MA). Uridine 5′-diphosphoglucuronic acid trisodium salt (UDPGA), calcein-AM, human recombinant TNF-α and 3-(4,5-dimethyl-2-thiazolyl)-2,5-diphenyl-2*H*-tetrazolium bromide (MTT) were purchased from Sigma Aldrich (St. Louis, MO). Phosphate buffered saline (PBS) was from Fisher Scientific S.L. (Madrid, Spain). Dimethyl sulfoxide (DMSO), diethyl-ether and high-performance liquid chromatography (HPLC) reagents, formic acid and acetonitrile (ACN), were obtained from Panreac (Barcelona, Spain). Methanol (MeOH) was from Lab-Scan (Gliwice, Poland). Ultrapure Millipore water was used for all solutions.

2.2 Enzymatic synthesis of urolithin A glucuronide

Uro-A-Gluc (3,8-dihydroxy-6H-dibenzo[b,d]pyran-6-one glucuronide) was synthesized as follows: the mixture (final volume 0.5 mL) containing PBS (pH 7.4), 1 mM UDPGA, 40 μM Uro-A and 0.5 mg/mL UGT1A1 was incubated at 37°C for 24 h. Control reactions in the absence of enzyme were carried out in parallel. At the end of the incubation, the reaction mix was filtered using Centricon Centrifugal Filters (Millipore Billerica, MA) to recover the active enzyme which was reused in up to four successive incubations. The protein concentration was determined using the Folin-based *DC* protein assay (BioRad, Barcelona, Spain). The remaining mixture containing the reaction product was acidified (formic acid, 1.5%, v/v) prior to addition of distilled water (0.25 mL) and diethyl ether (2 mL) per 0.5 mL of mixture. The mix was vigorously vortexed for 30 s, allowed to stand for 5 min at room temperature and centrifuged at 2894 × *g* for 5 min before the organic phase was removed. Extraction with diethyl ether was repeated 3 times to ensure extraction of unconjugated Uro-A. The acidified aqueous phase containing the Uro-A-Gluc was filtered through pre-activated reverse phase C-18 SEP-PAK cartridges (Waters Millipore, Billerica, MA) where the glucuronide was retained in the cartridge, eluted in 1 mL of MeOH, evaporated in a Speedvac® concentrator (Savant SPD 121P, Thermo Scientific, Waltham, MA) and the residue re-dissolved in DMSO.

2.3 HPLC–tandem mass spectrometry (MS/MS) analysis

Stock solutions (in DMSO) of the each of the urolithin glucuronides and of the aglycones were stored at −20°C until analysis using an HPLC–diode-array detection (DAD)–MS/MS system (1200 Series, Agilent Technologies). Prior to injection, samples were diluted in MeOH:H_2O (10:90) and filtered (0.45 μm). The HPLC system was equipped with a 150 mm × 0.5 mm id, 5 μm, reverse phase ZORBAX SB-C18 column from Agilent Technologies (Madrid, Spain) and an HTC Ultra mass detector in series (BrükerDaltonics, Bremen, Germany). Water:formic acid (99:1, v/v) and ACN were used as mobile phases A and B, respectively, with a flow rate of 10 μL/min. The linear gradient started with 1% of solvent B in solvent A, reaching 60% solvent B at 30 min and 90% at 31 min which was maintained up to 36 min. The initial conditions were re-established at 36.5 min and kept under isocratic conditions up to 43 min. The mass detector was an ion-trap mass spectrometer equipped with an electrospray ionization (ESI) system (capillary voltage, 4 kV; dry temperature, 350°C). MS and MS/MS daughter spectra were measured from m/z 100–1200 using the Ultra scan mode (26 000 $m/z/s$). Collision-induced fragmentation experiments were also performed using helium as collision gas, and the collision energy was set at 75%. MS data were acquired in the negative ionization mode. Urolithin glucuronides and urolithins were confirmed by their spectral properties, molecular mass and fragmentation pattern. Quantification of all these metabolites was made at 305 nm using the corresponding pure compounds as external standard. The parameters of the calibration functions: calibration range, linearity, limit of detection (LOD), limit of quantification (LOQ) and % of recovery are summarized in Supporting Information Table S1. All calibrations curves showed good linearity ($R^2 = 0.997$) in a wide range of concentrations (∼0.1–20.0 μM). The LOD was between 0.11 and 0.21 μM whereas the LOQ was between 0.53 and 0.70 μM. The estimated recovery percentages for each metabolite ranged from 89.9 to 109.8% indicating a good recovery of these compounds from the culture media. The proposed method has also good intra-day variability (relative standard deviation [RSD], ranged from 0.19 to 7.95 %) and inter-day variability (RSD from 0.13 to 14.91 %). Comparison between the standard curves for the synthesized Uro-A-Gluc and Uro-A showed that both metabolites exhibited similar response factors.

To determine the stability in the culture media of the glucuronides and of the aglycones during the treatments, cell culture supernatants were collected at the end of the experiment and analysed to measure the presence and concentration of the tested compounds. ACN (250 μL) was added per 100 μL of culture media, vortexed and centrifuged at 16 435 × *g* for 10 min. The supernatant was then concentrated in a Speedvac® concentrator (Savant SPD 121P) and the residue re-dissolved in 100 μL of MeOH, diluted in water (1:1) and filtered (0.45 μm) before analysis by HPLC–MS/MS using the same conditions described above.

2.4 Cell culture

Unless otherwise stated, human aortic endothelial cells (HAECs) were cultured in complete endothelial cell growth medium (ECGM) and sub-cultured using the recommended subculture reagent kit. Cells and media were all obtained from the European Collection of Cell Cultures (Salisbury, UK). Cells were routinely seeded at a density of 10^4 cells/cm^2 in 25-cm^2 flasks and maintained at 37°C in a humidified atmosphere at 5% of CO_2. The culture medium was changed every other day until cells reached ∼90% confluence. Cell cultures between three and seven passages were used for all the experiments. Human acute monocytic leukaemia THP-1 cells were also obtained from the European Collection of Cells Cultured (Salisbury, UK). Cells were maintained in RPMI 1640 culture media containing 10% fetal bovine serum, 2 mM L-glutamine, 100 U/mL penicillin and 100 μg/mL streptomycin (Gibco, Invitrogen S.A., Barcelona, Spain) at a final pH 7.2–7.4 and 37°C under a 5% CO_2/95% air atmosphere at constant humidity. Cells were seeded at 3–5 × 10^5 cells/mL on 75 cm^2 flasks (Nunc, Roskilde, Denmark) and sub-cultivated every 2 days (cell concentration in the culture media did never exceed 8 × 10^5 cells/mL). Cells passages between 15 and 30 were used for the experiments.

2.5 Cell adhesion assay

Monocyte adhesion to aortic endothelial cells was evaluated using the human leukaemia monocytic THP-1 cells. Cultured monocytes (1×10^6 cells/mL) were re-suspended in PBS and labelled with 5 μL/mL of calcein-AM (5 μM final concentration) for 30 min at 37°C. The cells were then centrifuged at 150 ×*g* for 5 min and washed twice with PBS before addition to the human aortic cells. HAECs were cultured in 96-well plates at a density of 10^4 cells/well until they reached confluence. An initial test with two concentrations of TNF-α (10 ng/mL and 50 ng/mL dissolved in culture medium and filtered through 0.22 μm prior adding to the cells) at two time points, 4 and 8 h, was carried out. The highest induction of monocyte adhesion to HAECs was observed using 50 ng/mL of TNF-α already after 4 h of incubation, and thus, these conditions were selected for investigating the effects of the metabolites on monocyte adhesion. The initial concentration of each compound in the culture media was established by direct HPLC analysis immediately after addition of the stock to the medium and were: 12.3 ± 0.3 μM Uro-A-Gluc, 18.5 ± 1.1 μM Uro-A, 20.4 ± 2.6 μM Uro-B-Gluc and 14.9 ± 0.5 μM Uro-B. Two more diluted concentrations were also tested (∼1.0 and ∼5.0 μM). Control cells were treated in parallel with the equivalent amount of DMSO (0.5 %). After treatment, the cells were washed twice with PBS and co-incubated with the calcein-labelled monocytes (2×10^5 cells per well) in the dark for 1 h at 37°C. Non-adhering cells were removed and the remaining cells washed twice with PBS before fluorescence was measured with a fluorescence-detecting microplate reader (Fluostar Galaxy, BMG Lab. Technologies v5.0, Cary, NC) using excitation at 492 nm and emission at 520 nm. Experiments were carried out in triplicate ($n = 6$ wells per treatment).

2.6 Migration assay

HAECs were cultured in 24-well plates at an initial density of 10^4 cells/cm^2. At confluency, a small area was disrupted and a group of cells destroyed or displaced by scratching a line horizontally through the monolayer with a sterile pipette tip. Media, dislodged cells and debris were aspirated and cells washed twice with PBS before the culture medium was replaced. The cells were then treated with the inflammatory cytokine TNF-α (50 ng/mL) and each of the tested metabolites at the same concentrations described for the adhesion assay. Control cells were treated in parallel with the equivalent amount of DMSO. The open gap was inspected microscopically over time as the cells moved in and filled the damaged area. Images were captured at the beginning (time 0) and at regular time points (every 4 h) during cell migration to a maximum of 24 h using a contrast inverted microscope and a charge-coupled device (CCD) camera attached to the microscope. Three selected views were photographed along the scraped area on each well. The average distance between the two sides of the gap was determined by measuring the distance (μm) between two points ($n = 10$ measurements) along each photographed area. We detected differences between experimental conditions (TNF-α alone vs. TNF-α + metabolite) after 12 h of treatment and thus final migrated distance was calculated as the difference between the gap distance at time 0 and time 12 h (at later time points, cells had grown too much into the gap and it was difficult to measure the distance between the two sides). Data are representative of three to four experiments ($n = 2$ wells per treatment).

2.7 Cell viability assay

Cell viability was estimated using the MTT assay [20]. HAECs were cultured and treated under the same conditions as described for the migration assay. At the end of the incubation time (12 h), the culture medium was replaced by 1 mL of MTT solution (1.0 mg/mL in serum-free ECGM) and incubated for a further 3 h. The formazan crystals formed in the viable cells were solubilized with DMSO (625 μL) and the optical density was measured at a test wavelength of 570 nm and a reference wavelength of 690 nm using a microplate reader (Fluostar Galaxy, BMG Lab. Technologies v5.0). Data are presented as mean values ± SD from three independent experiments ($n = 2$ wells per experiment).

2.8 Human antibody arrays

Changes in the expression levels of proteins involved in cell adhesion and cell migration were investigated using: (i) custom designed human antibody arrays containing 20 markers of adhesion and, (ii) human antibody membrane arrays RayBio® Human Growth Factor Array which contains 41 growth factors (RayBiotech, Inc., Norcross, GA) following the manufacturer's recommendations. The configuration of the antibody arrays is given in Supporting Information Figs. S1 and S2. HAECs were cultured in 6-cm plates at an initial density of 10^4 cells/cm^2. Confluent cells were treated with: (i) TNF-α (50 ng/mL), (ii) TNF-α + Uro-A-Gluc (∼15 μM) or (iii) TNF-α + Uro-A (∼15 μM) for 4 h (adhesion factors) or 12 h (migration factors). After treatment, cells were washed twice with PBS and lysed with 0.5 mL of ice-cold lysis RIPA buffer containing a cocktail of proteases inhibitors (Roche, Manhein, Germany). Lysates were centrifuged at 23 200 × *g* for 15 min at 4°C and frozen at −80°C until analysis. Cell lysates from two plates were pooled and the protein content was measured by the *DC* colorimetric assay at 750 nm (Bio-Rad, Barcelona, Spain) and based on a bovine serum albumin standard curve. Total equivalent amounts of protein (300 μg) were incubated with the arrays for 2 h at room temperature. Detection was performed with biotin-conjugated antibodies raised against the particular molecules and horseradish

peroxidase-conjugated streptavidin. Arrays were visualized using a CCD camera coupled to a Chemidoc 881XRS equipment (Biorad Laboratories, Barcelona, Spain). Non-saturated spots were scanned and converted to densitometric units using the software ScanAlyze (Stanford Computer Graphic Laboratory's, PaloAlto, CA) [21]. The proteins were represented in duplicates per array. Negative controls and blank spots were used to determine the background. Raw data (intensity value of each spot) were subtracted from the averaged background and normalized according to positive control densities. Differences in protein expression between experimental groups are expressed as fold-change. Proteins showing changes in expression $\geq$1.3-fold or $<$1.3-fold were considered as up-regulation or down-regulation, respectively (because modest changes in expression may have biological significance). Cell extracts from two plates were pooled and hybridized with the array. Duplicate experiments were performed for each treatment. Data are presented as the mean value $\pm$ SD.

2.9 Measurement of adhesion molecules, growth factors and cytokines by enzyme-linked immunosorbent assay (ELISA)

Confluent HAECs were cultured at an initial density of 10^4 cells/well (6-cm plates) and treated with TNF-α (50 ng/mL) and each of the tested metabolites (at the concentrations described) for 4 h (adhesion molecules) or 12 h (migration factors). After treatment, cell lysates were prepared as previously described and frozen at −80°C until analysis of the specific molecules using the following commercially available human ELISA kits: s-ICAM-1 (Bender MedSystems, Vienna, Austria), VCAM-1 (Gen-Probe, San Diego, CA), platelet-derived growth factor beta polypeptide (PDGF-BB; Peprotech, Rocky Hill, NJ) and β-type platelet-derived growth factor receptor (PDGF-R-β; Sino Biological, Schilde, Belgium). The minimum detection levels were 6.25 and 0.6 ng/mL for s-ICAM-1 and VCAM-1 and 62 and 62.5 pg/mL for PDGF-BB and PDGF-R-β, respectively. Data are presented as the mean value from three independent experiments (cell extracts from two plates were pooled per experiment). For the analysis of interleukin-8 (IL-8), CCL2 and plasminogen activator inhibitor-1 (PAI-1), HAECs were also cultured at an initial density of 10^4 cells/well (96-wells plates) in serum-free ECGM for 12 h followed by treatment with TNF-α (50 ng/mL) and each of the tested metabolites for a further 4 h. After treatment, cell culture supernatants were collected and frozen at −80°C until further analysis of the cytokines using commercially available ELISA kits from Peprotech (Rocky Hill, NJ). The minimum detection level was 8 pg/mL for IL-8 and CCL2 and 23 pg/mL for PAI-1. Protein concentration was determined by the DC protein assay using a microplate reader (Infinite M200, Tecan, Grodig, Austria). This assay was carried out at least in triplicate ($n = 6$ wells per experiment) and values are presented as the mean $\pm$ SD.

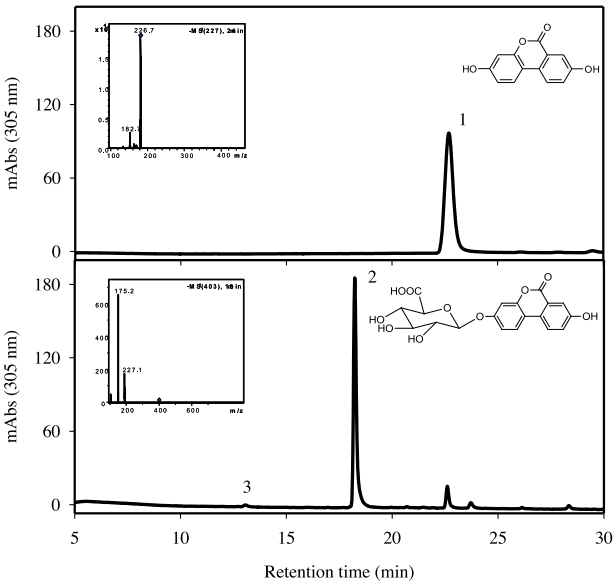

Figure 1. HPLC profiles (305 nm), structure and mass spectral properties of Urolithin A (Uro-A; m/z^- 227), peak 1 and Urolithin A glucuronide (Uro-A-Gluc; m/z^- 403, MS–MS m/z^- 227.1, 175.2), peak 2. A third peak (peak 3) indicating the presence of small quantities of Urolithin A diglucuronide (m/z^- 579.2, MS–MS m/z^- 402.9) is also indicated.

2.10 Statistical analyses

Results are presented as mean values $\pm$ SD (displayed as error bars). Where indicated, data were statistically analysed using PASW statistics 18.0 (SPSS Inc., Chicago, IL) and differences between experimental groups were made using two-tailed unpaired Student's *t*-test. Results with a *p*-value < 0.001, < 0.01 or < 0.05 were considered significant. Results showing a trend with *p*-values < 0.1 are also indicated.

3. Results

3.1 Enzymatic synthesis of urolithin A glucuronide

HPLC analysis of the reaction product after incubation of Uro-A with UGT1A1 in the presence of UDPGA for 24 h is shown in Fig. 1. Uro-A (peak 1) was mainly converted to one unique more polar product (peak 2). In LC–MS analysis operated in the negative ESI mode, this peak 2 exhibited an ion at m/z^- 403, which gave rise to fragment ions at m/z^- 227.1 and 175.2. Peak 2 also displayed an UV spectrum with three main absorption peaks at 348, 304 and 278 nm. These results indicated that the initial Uro-A was largely converted to a monoglucuronide derivative (Uro-A-Gluc) since no aglycone was detected in the final reaction product or in the organic phase (extracted with diethyl ether). Approximately 10% of this Uro-A-Gluc was lost in the organic phase. We did not detect any other monoglucuronide

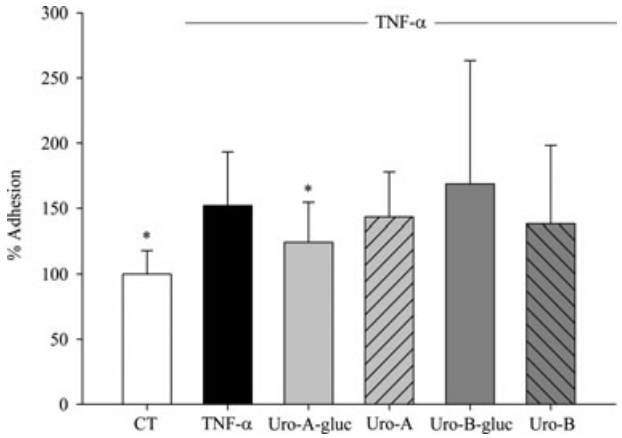

Figure 2. Effects of Uro-A-Gluc, Uro-B-Gluc and their respective aglycones, Uro-A and Uro-B, on TNF-α-stimulated adhesiveness of HAECs to THP-1 monocytes. HAECs were co-treated with TNF-α (50 ng/mL) and each of the metabolites (18.5 ± 1.1 μM Uro-A, 12.3 ± 0.3 μM Uro-A-Gluc, 14.9 ± 0.5 μM Uro-B and 20.4 ± 2.6 μM Uro-B-Gluc) for 4 h and adhesion to monocytes measured. The results from three separate experiments are expressed as mean percentage of untreated control ± SD. Symbols indicate differences from TNF-α-treated samples, $^{*}p < 0.05$.

throughout the chromatogram. However, we did detect a very small peak with a mass corresponding to the diglucuronide (peak 3; R_t: 12.8 min; m/z^-: 579.2, 402.9). Based on the UV absorbance, the relative percentage content of this diglucuronide was ∼2.5% that of the monoglucuronide. In the absence of enzyme (negative controls) the Uro-A was fully recovered with diethyl ether.

The stability of the glucuronides, Uro-A-Gluc and Uro-B-Gluc as well as of their corresponding aglycones, Uro-A and Uro-B, was monitored in the cell culture media after 4 and 12 h of incubation. HPLC–MS/MS analysis of the culture media indicated that all the metabolites tested were stable under the experimental conditions and that there was not hydrolysis of the glucuronides (Supporting Information Table S2).

3.2 Effect of the urolithin glucuronides and their aglycones on monocyte adhesion and cell migration of TNF-α-activated HAECs

To determine whether the urolithin glucuronides and (or) their aglycones exert any anti-inflammatory effects on the human vascular system, we first examined the effects of these metabolites on THP-1 monocytes adhesion and ECs migration in TNF-α-activated HAECs. Figure 2 shows that incubation of HAECs with TNF-α (50 ng/mL for 4 h) significantly increased the monocytes adhesiveness (52% increase, $p < 0.05$). Of the metabolites tested, Uro-A, Uro-B-Gluc and Uro-B did not show any effect on the monocytes adhesion and only the Uro-A-Gluc (at ∼15 μM concentration) was able to inhibit the monocytes adhesion to TNF-α-stimulated HAECs in a significant manner (∼30% inhibition, $p < 0.05$). We further tested whether the Uro-A-Gluc had any effect against monocyte adhesion at two lower concentrations (∼5 μM and 1 μM) but no inhibition was observed (results not shown).

The effect of TNF-α and of the glucuronides and their corresponding aglycones on the migration of HAECs is shown in Fig. 3. Endothelial cell migration was moderately induced after treatment with TNF-α for 12 h (∼20% induction, $p < 0.01$). Co-treatment of TNF-α with Uro-A-Gluc, Uro-A or Uro-B-Gluc (at ∼15 μM) decreased the migration distance back to control values, more significantly for Uro-A-Gluc and Uro-A ($p < 0.05$) than for Uro-B-Gluc ($p < 0.1$). Uro-B did not show a significant effect. At ∼5 μM concentration, only Uro-A-Gluc and Uro-B-Gluc inhibited TNF-α-induced migration (∼20%, $p < 0.05$ and $p < 0.1$, respectively) but no effect was detected at 1 μM concentration (results not shown). Neither the urolithins nor their glucuronides had any effect on HAECs migration in the absence of the inflammatory cytokine (data not shown). In order to determine if the urolithin metabolite treatments were inducing gross changes in the cells which may indicate some kind of toxicity of the treatments, the effects of the treatments on cell reductase enzyme activity were assessed using the MTT assay. None of the treatments caused significant changes in rates of MTT reduction, providing evidence that the cell responses to the urolithin metabolites were not likely to be due to gross toxic effects on the cells.

3.3 Antibody arrays

Since our results on the adhesion and migration assays were more significant for the Uro-A-Gluc and this compound is the metabolite most frequently detected in plasma [15, 16], we chose this compound for the subsequent study of the changes in adhesion cytokines and growth factors. In addition, Uro-A, which was effective at inhibiting migration, was also investigated for its modulatory effects on growth factors. We used human antibody arrays to screen for changes in the levels of expression of several key adhesion molecules and growth factors that may be associated to the response of the HAECs to TNF-α activation and to the modulatory effect of Uro-A-Gluc and Uro-A on the TNF-α-induced response. The complete profile of proteins represented on the arrays (ranked in order of spot intensity from highest to lowest value) and the differences detected for each one between the experimental groups (fold-change) are included in Supporting Information Table S3 (adhesion markers) and Supporting Information Table S4 (growth factors). A selection with the adhesion proteins and growth factors most markedly affected by the treatments is listed in Table 1. Densitometric analysis showed that the adhesion molecules CCL2, IL-8, SELE, ICAM-1 and the vascular cell adhesion molecule 1 (VCAM-1), several platelet-derived growth factors (PDGF-BB, PDGF-AB, PDGF-AA) and the receptors, insulin like growth factor 1 soluble receptor (IGF-I sR), β-type platelet-derived growth factor receptor (PDGF-R-β) and the stem cell growth receptor (SCF) were all

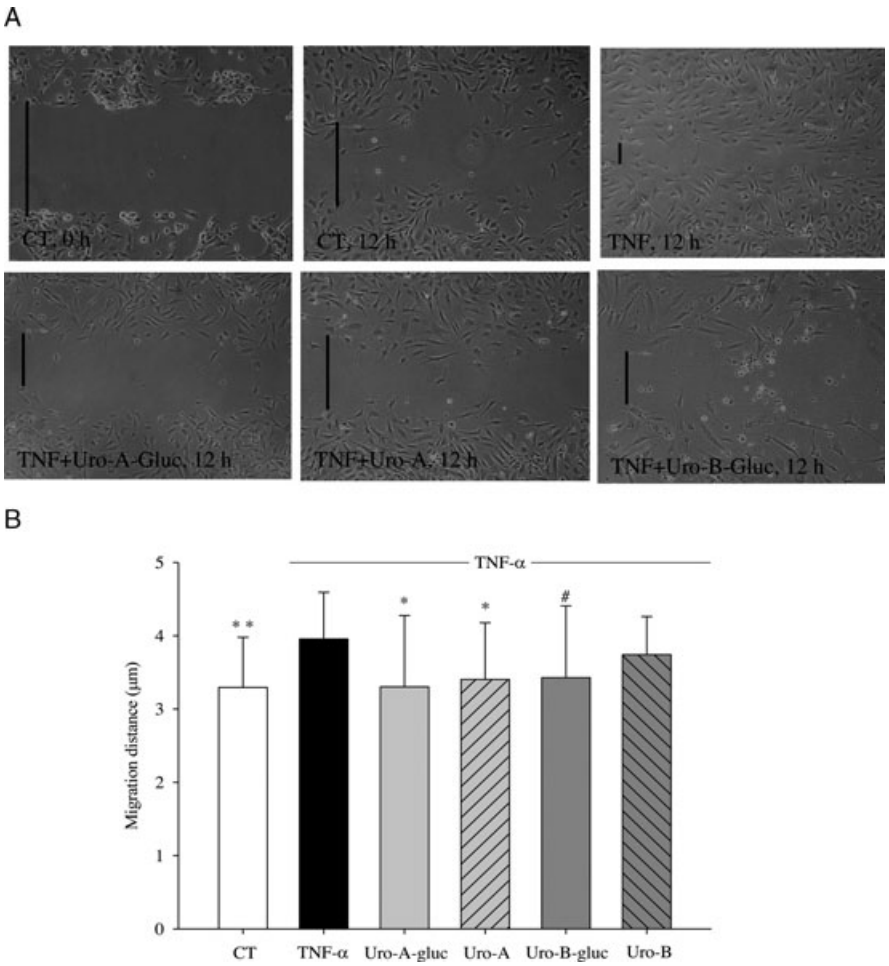

Figure 3. Effects of Uro-A-Gluc, Uro-B-Gluc and their respective aglycones, Uro-A and Uro-B, on TNF-α-stimulated migration of HAECs. HAECs were co-treated with TNF-α (50 ng/mL) and each of the metabolites (18.5 ± 1.1 μM Uro-A, 12.3 ± 0.3 μM Uro-A-Gluc, 14.9 ± 0.5 μM Uro-B and 20.4 ± 2.6 μM Uro-B-Gluc) for 12 h and migration distance determined. (A) Representative photomicrographs showing migration of HAECs in control medium at times 0 and 12 h. Effects of TNF-α alone in comparison to treatment with each metabolite on TNF-α-stimulated HAECs. (B) Histograms showing the final migrated distance calculated as the difference between the gap distance at time 0 and after 12 h of incubation. Data are representative of three to four experiments (mean value ± SD). Symbols indicate differences from TNF-α-treated samples, $^{\#}p < 0.1$, $^{*}p < 0.05$, $^{**}p < 0.01$.

up-regulated in HAECs following treatment with TNF-α. Of those, co-treatment with Uro-A-Gluc exhibited a tendency to down-regulate the levels of CCL2, PDGF-BB, PDGF-AB, PDGF-AA, PDGF-R-β, IGF-I sR and SCF. Uro-A was also able to significantly reduce the expression levels of PDGF-BB, PDGF-AB, PDGF-AA, IGF-I sR and SCF. In addition, some other proteins were found to be down-regulated following treatment with TNF-α: IGF-II, macrophage colony stimulating factor receptor (M-CSFR), glial cell line-derived neurotrophic factor (GDNF) and ICAM-2 and then up-regulated by co-exposure to Uro-A-glucuronide or its aglycone.

3.4 Effects on individual cytokines and growth factors using ELISAs

To further validate some of the antibody array results, we used ELISAs to measure the concentrations of selected chemokines, adhesion molecules and growth factors (Fig. 4). The results corroborated that stimulation of the HAECs with the pro-inflammatory cytokine TNF-α (50 ng/mL) for 4 h significantly ($p < 0.001$) up-regulated the expression of IL-8 (7.5-fold), CCL2 (9.7-fold), VCAM-1 (9.8-fold) and ICAM-1 (200-fold) (Fig. 4). Also, in agreement with the antibody array results, co-treatment of the inflamed aortic cells with Uro-A-Gluc confirmed that the levels of CCL2 released to the cell culture media were significantly reduced (0.5-fold, $p < 0.01$) in comparison to those in the cytokine-treated cells (Fig. 4) whereas the levels of IL-8 did not differ significantly from those in the TNF-α-treated cells (Fig. 4). The Uro-A-Gluc did not show, however, any effect on the levels of CCL2 at 5 μM or 1 μM concentrations. Furthermore, the expression levels of VCAM-1 and ICAM-1 were shown to be unmodified following treatment of cells with TNF-α and the Uro-A-Gluc (Fig. 4). We additionally tested the effects of Uro-A on the levels of IL-8 and CCL2 released into the cell culture media. The aglycone was also able to significantly reduce the levels of IL-8 (0.6-fold, $p < 0.05$) and CCL2 (0.7-fold, $p < 0.01$) (Fig. 4). In addition, Uro-A was able to down-regulate the levels of IL-8 at 5 μM concentration (0.75-fold, $p < 0.05$) but not of CCL2. TNF-α stimulation for 12 h also moderately

Table 1. Profile of most significant altered adhesion proteins and human growth factors expression in HAECs: (i) TNF-α-treated cells (TNF-α) *versus* control cells (CT), (ii) TNF-α + Uro-A glucuronide-treated cells (TNF-α + Uro-A-Gluc) *versus* TNF-α-treated cells and (iii) TNF-α + Uro-A-treated cells (TNF-α + Uro-A) *versus* TNF-α-treated cells and. Cut-off value: up-regulation fold-change ≥ 1.3, down-regulation fold-change < −1.3.

Protein		TNF-α/CT		TNF-α + Uro-A-Gluc/TNF-α		TNF-α + Uro-A/TNF-α	
Name	Symbol	Change (fold-change)	*p*-value[a]	Change (fold-change)	*p*-value	Change (fold-change)	*p*-value
High spot intensity (≥0.25)[b]							
Insulin-like growth factor II	IGF-II	Down-regulated (−1.92)[c]	0.155	Up-regulated (2.68)	0.002	N.C. (1.30)	–
Platelet-derived growth factor subunit B (homodimer)	PDGF-BB	Up-regulated (2.41)	0.148	Down-regulated (−3.06)	0.139	Down-regulated (−2.04)	0.005
Chemokine (C–C motif) ligand 2	CCL2	Up-regulated (7.71)	0.004	Down-regulated (−1.32)	0.068	N.A.	–
Interleukin-8	IL-8	Up-regulated (6.19)	0.083	N. C. (1.05)	–	N.A.	–
Endothelial leukocyte adhesion molecule 1, E-selectin	SELE	Up-regulated (5.96)	0.003	N. C. (1.06)	–	N.A.	–
Intercellular adhesion molecule 1	ICAM-1	Up-regulated (2.96)	0.052	N.C. (−1.28)	–	N.A.	–
Moderate spot intensity (<0.25 and >0.1)							
Platelet-derived growth factor subunit B (heterodimer)	PDGF-AB	Up-regulated (1.73)	–	Down-regulated (−2.38)	0.181	Down-regulated (−1.76)	0.015
Vascular cell adhesion molecule 1	VCAM-1	Up-regulated (5.57)	0.016	N.C. (−1.29)	–	N.A.	–
Low spot intensity (<0.1)							
Insulin-like growth factor 1 soluble receptor	IGF-I sR	Up-regulated (1.96)	–	Down-regulated (−2.56)	0.122	Down-regulated (−2.50)	0.068
Platelet-derived growth factor A chain	PDGF-AA	Up-regulated (1.63)	–	Down-regulated (−2.04)	0.161	Down-regulated (−2.04)	0.015
Beta-type platelet-derived growth factor receptor	PDGFR-β	Up-regulated (1.42)	–	Down-regulated (−1.61)	–	Down-regulated (−1.96)	0.095
Mast/stem cell growth factor	SCF	Up-regulated (2.55)	0.196	Down-regulated (−3.33)	0.054	Down-regulated (−2.17)	0.107
Macrophage colony-stimulating factor 1	M-CSF	N.C. (1.09)	–	Up-regulated (2.21)	0.024	N.C. (−1.11)	–
Macrophage colony stimulating factor receptor	M-CSFR	Down-regulated (−1.63)	0.136	Up-regulated (2.35)	0.003	N.C. (−1.28)	–
Glial cell line-derived neurotrophic factor	GDNF	Down-regulated (−2.85)	–	Up-regulated (2.43)	0.003	Up-regulated (2.54)	–
Neurotrophin-3	NT3	N.C. (−1.29)	–	Up-regulated (1.96)	0.035	N.C. (−1.13)	–
Intercellular adhesion molecule 2	ICAM-2	Down-regulated (−21.2)	0.004	Up-regulated (3.75)	–	N.A.	–

a) Cell extracts from two plates were pooled and hybridized onto one antibody array per experiment. Data are presented as the mean value from two independent experiments. Estimated *p*-values < 0.2 are indicated. N.C., not changed; N.A., not analysed.
b) Spot intensity was determined by densitometric analysis. Intensity value for each spot was subtracted from the averaged background and normalized to positive control densities. Proteins are ranked in order of intra-array normalized spot intensity from highest to lowest values.
c) (fold-change)

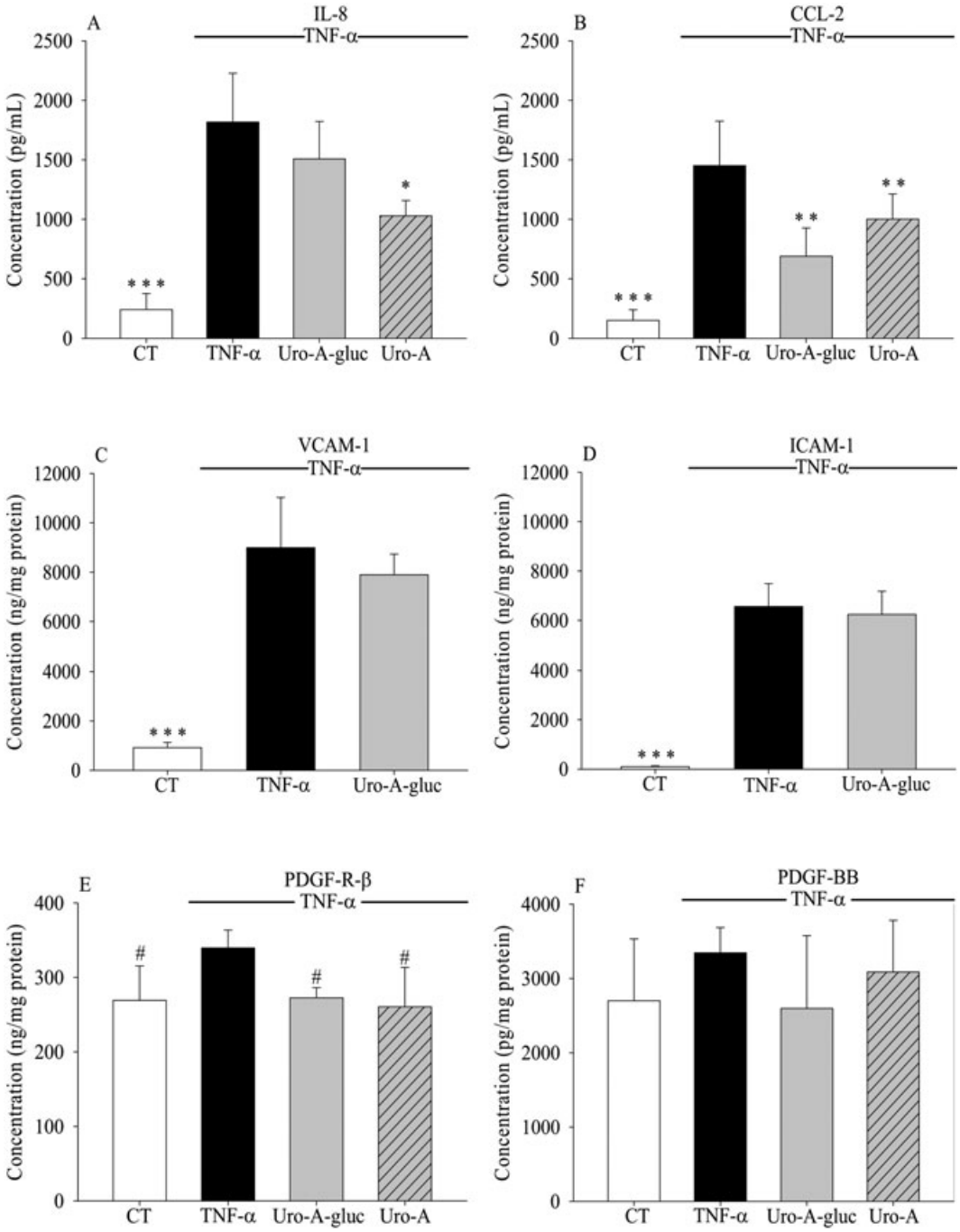

Figure 4. Levels of selected cytokines and growth factors as measured by ELISA assays in the supernatants or cell extracts from HAECs exposed to TNF-α (50 ng/mL) and each of the metabolites (12.3 ± 0.3 μM Uro-A-Gluc, 18.5 ± 1.1 μM Uro-A). (A) and (B) IL-8 and CCL2 released to the cell culture media after 4 h of treatment; (C) and (D) expression levels of VAM-1 and ICAM-1 in HAECs extracts after 4 h of treatment; (E) and (F) expression levels of PDGFBB and PDGF-R-β in HAECs extracts after 12 h of treatment. Data are presented as the mean value from three independent experiments ± SD. Cell extracts from two plates were pooled per experiment. Symbols indicate differences from TNF-α-treated samples, $^{\#}p < 0.1$, $^{*}p < 0.05$, $^{**}p < 0.01$, $^{***}p < 0.001$.

induced the levels of PDGF-R-β (1.3-fold, $p < 0.1$) which were slightly down-regulated (0.75-fold) by Uro-A-Gluc and Uro-A ($p < 0.1$) (Fig. 4). No significant changes were observed in thelevels of PDGF-BB (Fig. 4). In addition to the selected markers we also investigated the changes in the levels of PAI-1 which was also highly up-regulated (4.5-fold) after treatment with the cytokine ($P < 0.001$) and marginally down-regulated by the Uro-A-Gluc (0.8-fold, $P < 0.01$) (Fig. 5).

4 Discussion

The link between the cardioprotective effects of dietary polyphenols and the actual molecules responsible for them has not been yet clearly established. This is due in part to remaining unanswered questions on critical issues: (i) the full identification and quantification of the metabolites found in vivo after the intake of polyphenols; (ii) the specific tissue distribution and the molecular mechanisms triggered in the cells by these molecules [13]. In the present work, we have addressed these two key points by investigating some of the anti-inflammatory effects and potential underlying molecular mechanisms of the main in vivo plasma metabolites derived from dietary ETs, Uro-A-Gluc and Uro-B-Gluc, as well as of their respective aglycones, against cells of the vascular system. Among the tested metabolites, Uro-A-Gluc, at low μM concentrations (∼5–15 μM), inhibited monocyte adhesion and endothelial cell migration in a significant manner. These effects were associated with a moderate but significant down-regulation of the levels of CCL2 and PAI-1. The aglycone, Uro-A, also inhibited endothelial cell migration but not monocyte adhesion and was able to down-regulate the expression levels of CCL2 and IL-8.

The possibility of the polyphenol-derived metabolites being the bioactive molecules has only been scarcely explored due to the lack of authentic specimens of the compounds in sufficient quantities for research purposes as well as the difficulty and cost of synthesizing them. Increasing reports are now appearing looking at the synthesis of animal and human polyphenol conjugates mostly using multistep complex chemical methods which often yield mixtures of metabolites and request further chromatographic purification [22, 23]. In contrast, the use of enzymatic synthesis has been less explored. Mixed quercetin glucuronides were tentatively produced using cell-free pig liver extract and UDP-glucuronic acid [24]. More recently, recombinant human UDP-glucuronosyl transferases (UGTs) were used to efficiently glucuronidate several fungal metabolites. Among the tested UGTs, UGT1A1 exhibited the highest activity against these substrates [25]. These results prompted us to apply this approach to the synthesis of Uro-A-Gluc. We compared the glucuronidation of Uro-A between UGT1A1 and UGT1A10 and found that, under the same incubation conditions, UGT1A10 was less efficient than UGT1A1 at producing the conjugate (data not shown). As shown by the HPLC profile, UV spectrum and mass spectral properties [26], the principal detected product was a glucuronide derivative of Uro-A. The enzymatic method reported here enabled us to easily produce enough quantities of the metabolite for analytical purposes as well as for testing its bioactivity in cell culture studies (a starting quantity of ∼3.0 mg Uro-A produced ∼4.6 mg of Uro-A-Gluc, ∼87% yield). We assigned the 3 position to the synthesized monoglucuronide (Fig. 1) since the other physiologically relevant metabolite, Uro-B-Gluc, is the 3-glucuronide. However, the exact position of the glucuronic acid moiety (either 3- or 8-position) in the Uro-A-Gluc is not yet known. We have recently synthesized Uro-A-Gluc by a chemical method (results not shown). According to the NMR spectrum, the product was a mixture of the two regioisomers, Uro-A-3-Gluc and Uro-A-8-Gluc. Both compounds co-eluted in a single peak, with the same retention time and identical UV and MS/MS spectra. However, we have not succeeded yet in the chromatographic separation of the two compounds. Also, the Uro-A-Gluc detected previously in plasma and urine samples from animal and human studies [14–16] exhibit exactly the same chromatographic properties as the chemically and enzymatically synthesized compounds. Therefore, we cannot discard that the enzymatically synthesized compound may actually be a mixture of the two possible monoglucuronides.

The inhibition of the functions of the pro-inflammatory cytokine TNF-α and, in particular, the reduction of the monocyte adhesion to ECs is a key mechanism in the control of inflammation and plaque formation [8]. Our results indicate that exposure of the HAECs to the ET-derived metabolite Uro-A-Gluc, at low μM concentrations (∼15 μM), is associated with a modest but significant reduction of the TNF-α-induced adhesion of monocytes to cultured HAECs. The recent 'outside-in' theory which initiates the inflammatory response in the adventitia is supported by increased *vasa vasorum* neovascularization in the intima lesions and atheroma plaque [8]. Whereas pro-angiogenic molecules such as VEGF and TNF-α are associated to the growth of intimal lesions, anti-angiogenic molecules have proven to be effective inhibitors of *vasa vasorum* density and atheroma plaque development [27]. EC migration is an essential component of angiogenesis and is regulated by different cytokines, including growth factors, angiopoietins, interleukins and TNF-α [9]. In the present study, we have shown that the TNF-α-induced migration of HAECs was reduced following 12 h of exposure to some of the ET-derived metabolites, more significantly to Uro-A-Gluc and Uro-A, suggesting a moderate anti-angiogenic effect for these compounds.

The anti-inflammatory and anti-angiogenic effects exerted by the ET metabolites were found to be associated to modest changes in the expression levels of specific molecular markers involved in these processes as shown by antibody arrays and ELISA assays. Although antibody array technology has improved substantially over the past years, it is still very expensive and thus, it limits the number of replicates that can be performed. Like in other array technologies (i.e., gene expression microarrays), antibody arrays such as those used in our study are generally used as a semi-quantitative screening and need further validation by other techniques. RayBio antibody arrays have been recently reported to generate reproducible data with low intra-array coefficient of variation and high correlation between replicate experiments [28] and have also been efficiently validated by ELISA assays [28, 29]. Accordingly, we used several ELISA assays to confirm some of our arrays results. Under our experimental conditions, TNF-α-induced monocyte adhesion to HAECs was concomitant with the up-regulation of IL-8 and CCL2 as well as of ICAM-1

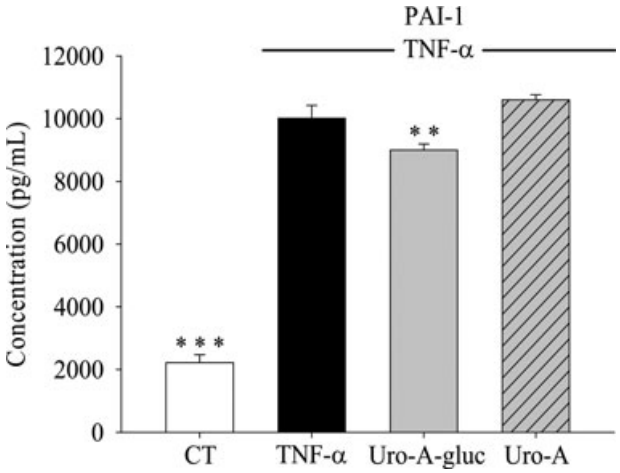

Figure 5. Levels of PAI-1 as measured by ELISA assay in the cell culture media from HAECs exposed to TNF-α (50 ng/mL) and each of the metabolites (12.3 ± 0.3 μM Uro-A-Gluc, 18.5 ± 1.1 μM Uro-A) for 4 h. Data are presented as the mean value from three independent experiments ± SD. Symbols indicate differences from TNF-α-treated samples, $^{**}p < 0.01$, $^{***}p < 0.001$.

and VCAM-1. The Uro-A-Gluc which effectively reduced the monocytes adhesion did not have any effect on the adhesion molecules or IL-8 but down-regulated the expression of CCL2 in a significant manner. All these results were shown both by antibody arrays and ELISA analyses. Using ELISA assays we also showed that Uro-A significantly down-regulated the levels of CCL2, a key regulator of monocytes migration highly expressed in atherosclerosis [30], and of IL-8, also an important chemoattractant cytokine for lymphocytes and a potent regulator of inflammation-induced angiogenesis [9, 10]. In addition, our antibody array results showed that PDGFBB, PDGFAB and PDGFAA, the three isoforms members of the PDGF family were all up-regulated in HAECs by the inflammatory cytokine TNF-α and down-regulated after exposure to Uro-A-Gluc or Uro-A. PDGFs bind to two different transmembrane tyrosine kinase receptors, PDGFR-α and PDGFR-β activating the downstream signalling pathway [31]. In particular, PDGFBB has been reported to enhance the growth and migration of ECs [32] and to propagate its mitogenic signals through binding and phosphorylation of its cognate receptor, PDGFR-β [33]. We further showed by ELISA assays that the levels of PDGFR-β were slightly up-regulated in TNF-α-inflamed HAECs and then reduced to control values by treatment with Uro-A-Gluc and Uro-A, although these results did not reach significance. Our results show, in general, good agreement between the RayBio antibody arrays used in this study and the ELISA assays. However, we were not able to detect changes in the levels of PDGF-BB using the ELISA technique which may be caused by differences between the antibodies used in the array and those selected for the ELISA assay.

Uro-A-Gluc was also able to significantly reduce the levels of TNF-α-induced PAI-1, a potent regulator of both vascular cell migration and of angiogenesis [34]. Elevated levels of PAI-1 are associated to atherosclerotic lesion and expression of PAI-1 is increased by inflammatory stimuli and decreased by drugs such as the statins used in patients with cardiovascular diseases (CVDs) [35]. Taken together, these results indicate that Uro-A-Gluc, one of the most abundant and most frequently detected metabolites in plasma after the intake of ET-containing foods, ameliorates the inflammatory response in human aortic endothelial cells by reducing the adhesion of monocytes, the migration of endothelial cells and regulating the levels of several chemotactic and angiogenic markers, in particular, of CCL2 and PAI-1. Under the conditions tested (low μM concentrations) these changes were all moderate.

There is an increasing number of in vitro studies in the literature looking at the putative role against CVDs of polyphenols at conditions more representative of the in vivo situation following the dietary intake of these compounds, i.e., testing low μM concentrations of the circulating plasma metabolites against cells of the vascular system. Like this, the effects of quercetin and some of its main conjugates, in particular, quercetin-3-glucuronide (Q3GA) on endothelial cells, vascular smooth muscle cells or macrophages under inflammatory conditions have been reported [36–40]. Although these studies have been carried out using different cell types and under different conditions and (or) treatment with the metabolites, it does appear that, in general, the aglycone quercetin was more efficient at decreasing the levels of the adhesion molecules such as ICAM-1 and VCAM-1 as well as of CCL2 than the Q3GA. However, some moderate responses have also been described for the glucuronide conjugate of quercetin [40]. Although it is difficult to extrapolate these data to the in vivo situation, overall, our results and others support the hypothesis that long-term consumption of polyphenols-containing foods may maintain a certain level (low μM concentrations) of their main derived metabolites circulating in plasma and that these metabolites may enter and interact with the aortic tissue. Indeed, some polyphenol conjugates such as Q3GA and resveratrol glucuronide have been localized in the aortic tissue [37, 41]. The metabolites may then modulate some of the cellular processes that lead to atherosclerosis and reduce the risk of developing this disease.

J.A.G. and M.L. are holders of a pre-doctoral JAE grant and a JAE-DOC contract from CSIC (Spain), respectively. This was funded by the Projects Consolider Ingenio 2010, CSD2007-00063 (Fun-C-Food), Fundación Seneca de la Región de Murcia, Spain (Grupo de Excelencia GERM 06 04486 and 05556/PI/04) and CICYT (ALG2011-22447).

The authors have declared no conflict of interest.

5 References

[1] Villablanca, A. C., Jayachandran, M., Banka, C., Atherosclerosis and sex hormones: current concepts. *Clin. Sci.* 2010, *119*, 493–513.

[2] Libby, P., Ridker, P. M., Hansson, G. K., Progress and challenges in translating the biology of atherosclerosis. *Nature* 2011, *473*, 317–325.

[3] Esper, R. J., Nordaby, R. A., Vilariño, J. O., Paragano, A. et al., Endothelial dysfunction: a comprehensive appraisal. *Cardiovasc. Diabetol.* 2006, *5*, 1–18.

[4] Becker, B. F., Heindl, B., Kupatt, C., Zahler, S., Endothelial function and hemostasis. *Z. Kardiol.* 2000, *89*, 160–167.

[5] Sprague, A. H., Khalil, R. A., Inflammatory cytokines in vascular dysfunction and vascular disease. *Biochem. Pharmacol.* 2009, *78*, 539–552.

[6] Bradley, J. R., TNF-mediated inflammatory disease. *J. Pathol.* 2008, *214*, 149–160.

[7] Zhang, H., Park, Y., Wu, J., Chen, X. et al., Role of TNF-α in vascular dysfunction. *Clin. Sci.* 2009, *116*, 219–230.

[8] Zagorchev, L., Mulligan-Keboe, M. J., Advances in imaging angiogenesis and inflammation in atherosclerosis. *Thromb. Haemost.* 2011, *105*, 820–827.

[9] Yoshida, S., Ono, M., Shono, T., Izumi, H. et al., Involvement of Interleukin-8, vascular endothelial growth factor, and basic fibroblasts growth factor in tumor necrosis factor alpha-dependent angiogenesis. *Mol. Cell. Biol.* 1997, *17*, 4015–4023.

[10] Szekanecz, Z., Shah, M. R., Harlow, L. A., Pearce, W. H. et al., Interleukin-8 and tumor necrosis factor-alpha are involved in human aortic endothelial cell migration. *Pathobiology* 1994, *62*, 134–139.

[11] Schiffrin, E. L., Antioxidants in hypertension and cardiovascular disease. *Mol. Interv.* 2010, *10*, 354–362.

[12] Larrosa, M., García-Conesa, M. T., Espín, J. C., Tomás-Barberán, F. A., Ellagitannins, ellagic acid and vascular health. *Mol. Aspects Med.* 2010, *31*, 513–539.

[13] Kaway, Y., Immunochemical detection of food-derived polyphenols in the aorta: macrophages as a major target underlying the anti-atherosclerosis activity of polyphenols. *Biosci. Biotechnol. Biochem.* 2011, *75*, 609–617.

[14] Espín, J. C., González-Barrio, R., Cerdá, B., López-Bote, C. et al., Iberian pig as a model to clarify obscure points in the bioavailability and metabolism of ellagitannins in humans. *J. Agric. Food Chem.* 2007, *55*, 10476–10485.

[15] Cerdá, B., Espín, J. C., Parra, S., Martínez, P. et al., The potent in vitro antioxidant ellagitannins from pomegranate juice are metabolised into bioavailable but poor antioxidant hydroxy-6H-dibenzopyran-6-one derivates by the colonic microflora of healthy humans. *Eur. J. Nutr.* 2004, *43*, 205–220.

[16] González-Sarrías, A., Giménez-Bastida, J. A., García-Conesa, M. T., Gómez-Sánchez, M. B. et al., Occurrence of urolithins, gut microbiota ellagic acid metabolites and proliferation markers expression response in the human prostate gland upon consumption of walnuts and pomegranate juice. *Mol. Nutr. Food Res.* 2010, *54*, 311–322.

[17] Larrosa, M., González-Sarrías, A., Yánez-Gascón, M. J., Selma, M. V. et al., Anti-inflammatory properties of a pomegranate extract and its metabolite urolithin-A in a colitis rat model and the effect of colon inflammation of phenolic metabolism. *J. Nutr. Biochem.* 2010, *21*, 717–725.

[18] González-Sarrías, A., Larrosa, M., Tomás-Barberán, F. A., Dolara, P. et al., NF-kappaB-dependent anti-inflammatory activity of urolithins, gut microbiota ellagic acid-derived metabolites, in human colonic fibroblasts. *Br. J. Nutr.* 2010, *104*, 503–512.

[19] Lucas, R., Alcantara, D., Morales, J. C., A concise synthesis of glucuronide metabolites of urolithin-B, resveratrol, and hydroxytyrosol. *Carbohydr. Res.* 2009, *344*, 1340–1346.

[20] van Meerloo, J., Kaspers, G.J., Cloos, J., Cell sensitivity assays: the MTT assay. *Methods Mol. Biol.* 2011, *731*, 237–45.

[21] Eisen, M. B., Brown, P. O., DNA arrays for analysis of gene expression. *Methods Enzymol.* 1999, *303*, 179–205.

[22] Fumeaux, R., Menozzi-Smarrito, C., Stalmach, A., Munari, C. et al., First synthesis, characterization, and evidence for the presence of hydroxycinnamic acid sulphate and glucuronide conjugates in human biological fluids as a result of coffee consumption. *Org. Biomol. Chem.* 2010, *8*, 5199–5211.

[23] González-Manzano, S., González-Paramás, A., Santos-Buelga, C., Dueñas, M., Preparation and characterization of catechin sulfates, glucuronides, and methylethers with metabolic interest. *J. Agric. Food Chem.* 2009, *57*, 1231–1238.

[24] O'Leary, K. A., Day, A. J., Needs, P. W., Sly, W. S. et al., Flavonoid glucuronides are substrates for human liver β-glucuronidase. *FEBS Lett.* 2001, *503*, 103–106.

[25] Pfeiffer, E., Hildebrand, A., Mikula, H., Metzler, M., Glucuronidation of zearalenone, zeranol and four metabolites in vitro: formation of glucuronides by various microsomes and human UDP-glucuronosyltransferase isoforms. *Mol. Nutr. Food Res.* 2010, *54*, 1468–1476.

[26] González-Barrio, R., Truchado, P., Ito, H., Espín, J. C. et al., UV and MS identification of urolithins and nasutins, the bioavailable metabolites of ellagitannins and ellagic acid in different mammals. *J. Agric. Food Chem.* 2011, *59*, 1152–1162.

[27] Gössl, M., Herrmann, J., Tang, H., Versari, D. et al., Prevention of vasa vasorum neovascularization attenuates early neointima formation in experimental hypercholesterolemia. *Basic Res. Cardiol.* 2009, *104*, 695–706.

[28] Li, Y., Flores, R., Yu, A., Okcu, M. F. et al., Elevated expression of CXC chemokines in pediatric osteosarcoma patients. *Cancer* 2011, *5*, 207–217.

[29] Wang, C., Peyron, P., Mestre, O., Kaplan, G. et al., Innate immune response to *Mycobacterium tuberculosis* Beijing and other genotypes. *PLoS One* 2010, *5*, 1–8.

[30] Deshmane, S., Kremlev, S., Amini, S., Sawaya, B. E., Monocyte chemoattractant protein 1 (MPC-1): an overview. *J. Interferon Cytokine Res.* 2009, *29*, 313–326.

[31] Barrientos, S., Stojadinovic, O., Golinko, M. S., Brend, H. et al., Growth factors and cytokines in wound healing. *Wound Rep. Reg.* 2008, *16*, 585–601.

[32] Imanishi, J., Kamiyama, K, Iguchi, I., Kita, M. et al., Growth factors: importance in wound healing and maintenance of transparency of the cornea. *Prog. Retin. Eye Res.* 2000, *19*, 113–129.

[33] Takimoto, T., Suzuki, K., Arisaka, H., Murata, T. et al., Effect of N-(*p*-coumaroyl) serotonin and N-feruloylserotonin, ma-

jor anti-atherogenic polyphenols in safflower seed, on vasodilation, proliferation and migration of vascular smooth muscle cells. *Mol. Nutr. Food Res.* 2011, *55*, 1–11.

[34] Stefansson, S., McMahon, G. A., Petitclerc, E., Lawrence, D. A., Plasminogen activator inhibitor-1 in tumor growth, angiogenesis and vascular remodelling. *Curr. Pharm. Des.* 2003, *9*, 1545–1564.

[35] Kruithof, E. K. O., Regulation of plasminogen activator inhibitor type I gene expression by inflammatory mediators and statins. *Thromb. Haemost.* 2088, *100*, 969–975.

[36] Tribolo, S., Lodi, F., Connor, C., Suri, S. et al., Comparative effects of quercetin and its predominant human metabolites on adhesion molecule expression in activated human vascular endothelial cells. *Atherosclerosis* 2008, *197*, 50–56.

[37] Ishizawa, K., Yoshizumi, M., Kawai, Y., Terao, J. et al., Pharmacology in health food: Metabolism of quercetin in vivo and its protective effect against arteriosclerosis. *J. Pharmacol. Sci.* 2011, *115*, 466–470.

[38] Winterbone, M. S., Tribolo, S., Needs, P. W., Kroon, P. A. et al., Physiologically relevant metabolites of quercetin have no effect on adhesion molecule or chemokine expression in human vascular smooth muscle cells. *Atherosclerosis* 2009, *202*, 431–438.

[39] Suri, S., Taylor, M. A., Verity, A., Tribolo, S., A comparative study of the effects of quercetin and its glucuronide and sulphate metabolites on human neutrophil function in vitro. *Biochem. Pharmacol.* 2008, *76*, 645–653.

[40] Al-Shalmani, S., Suri, S., Hughes, D. A., Kroon, P. A., Quercetin and its principal metabolites, but not myricetin, oppose lipopolysaccharide-induced hyporesponsiveness of the porcine isolated coronary artery. *Br. J. Pharmacol.* 2011, *162*, 1485–1497.

[41] Azorín-Ortuño, M., Yañez-Gascón, M. J., Vallejo, F., Pallarés, F. J. et al., Metabolites and tissue distribution of resveratrol in the pig. *Mol. Nutr. Food Res.* 2011, *55*, 1154–1168.

